Journal of Water Process Engineering 82 (2026) 109489

Contents lists available at ScienceDirect

Journal of Water Process Engineering

journal homepage: www.elsevier.com/locate/jwpe

Novel membrane-based PVDF modified by Na_2SiO_3 tested for water electrolysis systems

Soheyb Khadraoui [a,*], Kamel Noufel [a], Laid Telli [a], Alberto Figoli [b]

[a] Laboratory of Inorganic Materials, University Pole, Road Bourdj Bou Arreiridj, M'sila, 28000, Algeria
[b] Institute on Membrane Technology (ITM-CNR), Via P. Bucci 17/c, 87036, Arcavacata di Rende, CS, Italy

ARTICLE INFO

Editor: Tzyy Haur Chong

Keywords:
Ion exchange membranes
PVDF
Dual electrolyte
Water electrolysis

ABSTRACT

The present study investigates a significant advance in the development of ion exchange membranes (IEMs) for water electrolysis. A membrane based on polyvinylidene fluoride (PVDF) was modified through a simple and cost-effective process, consisting of the incorporation of 15 wt% sodium metasilicate (Na_2SiO_3), followed by an alkaline (NaOH) surface treatment to improve its hydrophilic and ionic properties (M3A). Advanced characterisation techniques were applied to the membrane. The (FTIR) analysis displays the presence of the various functional groups such as -OH, CH_2 (sp^3), CF_2, and Si-O-Si, while the (SEM) imaging showed a homogeneous surface. The membrane exhibited a tensile strength of 45.6 MPa. The ionic conductivity (IC), measured by electrochemical impedance spectroscopy (EIS), reached a value of 2.2×10^{-2} S/cm in 1 M of NaCl solution, while the ionic permeability showed a value of 1.78×10^{-4} cm/s for ions (Na^+), and 2.84×10^{-5} cm/s for protons (H^+). The water uptake observed was 24.8%, along with an ion exchange capacity (IEC) of 0.56 meq/g. Moreover, a remarkable permselectivity of 95% determined by the potentiometry technique was obtained, confirming the membrane's effectiveness in ionic separation. The application of M3A in water electrolysis was studied using chronopotentiometry (CP). The electrolysis voltage in a cell with two compartments of different pH is less than 1.5 V and demonstrated operational stability over 50 h. In this type of electrolysis, M3A ensures continuity of electric current flow by migration and prevents the chemical diffusion of protons. Compared to the commercial CMI-7000 membrane, M3A offers remarkable performance in water electrolysis.

1. Introduction

Polymeric membranes (PMs) are of significance in a variety of scientific and industrial applications, including gas separation, water treatment, and electrochemical systems. This is due to their design flexibility, tuneable properties, and low cost [1]. Recently various precursors have been used to produce PMs for instance poly(methyl methacrylate) PMMA, polysulfone PSU, poly(ether sulfone) PES, polyamide PA, polyimide PI, poly(vinylidene fluoride) PVDF, and poly(tetrafluoroethylene) PTFE [2]. Depending on their function, PMs are classified into filtration membranes (MF, UF, NF, RO), membrane distillation (MD), and ion-exchange membranes (IEMs) [3–5]. Among these, IEMs stand out for their ability to selectively transport ions while separating compartments—an essential feature in electrochemical processes [6]. IEMs are divided into cation-exchange membranes (CEMs), which conduct cations (e.g., H^+, Na^+) via fixed anionic groups like $–SO_3^-$, and anion-exchange membranes (AEMs), which transport anions (e.g., OH^-) through cationic groups such as $–NH_4^+$ [7,8]. Notable examples include Nafion 117 (a CEM) and various AEMs used in electrolysis and energy conversion [9,10].

From an environmental and energy perspective, ion-exchange membranes (IEMs) are critical components in water electrolysis (WE), as their ionic selectivity and conductivity directly govern system efficiency and hydrogen purity [11,12]. It exists various technology of WE, including alkaline water electrolysis (AWE), proton exchange membrane water electrolysis (PEMWE), and solid oxide electrolysis cells (SOEC) [12,13]. AWE approach is the most widely implemented electrolysis technology at the industrial scale, owing to its cost-effective design and compatibility with inexpensive, readily available materials [14]. One of the main challenges of AWE is the high energy consumption, where the theoretical minimum thermodynamic potential applied (1.23 V at pH 14 and 25 °C) is predicted by the Nernst equations [15,16]. This potential corresponds to the following oxidation-reduction reactions:

* Corresponding author.
E-mail address: soheyb.khadraoui@univ-msila.dz (S. Khadraoui).

https://doi.org/10.1016/j.jwpe.2026.109489
Received 5 October 2025; Received in revised form 25 November 2025; Accepted 8 January 2026

$$2H_2O + 2e^- \rightarrow H_{2(g)} + 2OH^- \quad (1)$$

$$E_{H_2O/H_2} = -0.83 \text{ V vs.SHE (at pH} = 14)$$

$$4OH^- \rightarrow O_{2(g)} + 2H_2O + 4e^- \quad (2)$$

$$E_{O_2/OH^-} = +0.40 \text{ V vs.SHE (at pH} = 14)$$

On the other hand, an innovative approach to reduce energy consumption in water electrolysis is the dual-electrolyte (DE) configuration, which enables independent optimization of anodic (alkaline) and cathodic (acidic) reaction environments. This asymmetric setup can lower energy demand by up to ~68% compared to conventional systems [17]. By using a concentrated basic medium (NaOH or KOH solution) at the positive electrode and a strong acidic medium (H_2SO_4 solution) at the negative electrode, the applied voltage drops from 1.23 V (standard theoretical value) to 0.4 V [16,18]. This significant energy gain can be attributed to the following factors:

- Cathodic compartment

$$2H^+ + 2e^- \rightarrow H_{2(g)} \quad (3)$$

$$E_{H^+/H_2} = 0 \text{ V vs.SHE (at pH} = 0)$$

- Anodic compartment

$$4OH^- \rightarrow O_{2(g)} + 2H_2O + 4e^- \quad (4)$$

$$E_{O_2/OH^-} = +0.40 \text{ V vs.SHE (at pH} = 14)$$

The efficiency of the DE electrolysis technique depends on the use of electrodes with high resistance to corrosion and chemically stable membranes in aggressive environments [19]. In this respect, researchers are focusing in particular on the use of bipolar membranes (BPM) and proton exchange membranes (PEMs), which are widely employed in electrolysis processes [20–22]. From the literature, both bipolar membranes (BPMs) and perfluorinated proton-exchange membranes (PEMs) exhibit significant limitations for practical dual-electrolyte water electrolysis. For instance, Lee et al. [18] reported a BPM based on poly(aryl ether ketone) (PAEK) that required a relatively high cell voltage of 1.59 V at a low current density of only 20 mA cm^{-2}. Such performance is unsuitable for industrial-scale hydrogen production, which typically demands current densities ≥100 mA cm^{-2} with minimal voltage overhead. On the other hand, Ming-Yuan Lin et al. [16] employed Nafion 211, a commercial PEM, in a KOH/H_2SO_4 DEWE system and achieved enhanced hydrogen evolution (0.95 L h^{-1}). However, Nafion membranes are prohibitively expensive, limiting their scalability. Moreover, under comparable operating conditions, Nafion 211 in their tests required ~2.0 V to reach 100 mA cm^{-2} at 25 °C. To overcome these limitations, an important and widely used polymer material is PVDF, which has attracted significant interest from researchers. This polymer is distinguished by its exceptional properties, particularly its high thermal, chemical stability and low cost. However, due to its insulating nature and high hydrophobicity, PVDF requires specific modifications to be used in the production of IEMs for electrochemical applications [23]. These adaptations aim to improve its IC and hydrophilicity properties to optimise its performance in a variety of electrolytic environments [24]. To enhance the intrinsic properties of PVDF, specifically its IC and hydrophilicity, various approaches have been employed, including energetic irradiation, polymer blending, the use of comb-branched copolymers, incorporation of dopants (such as nanomaterials and ionic liquids), addition of inorganic fillers, and surface treatments [25–27]. While PVDF membranes have been used in single-electrolyte water electrolysis (e.g., Sarthak et al. [28]), their application in dual-electrolyte systems remains scarce and underexplored. This present work aims to produce an efficient, cost-effective, and easily prepared IEM from polyvinylidene fluoride (PVDF) modified by sodium metasilicate (Na_2SiO_3). The produced IEM was characterised in terms of both physicochemical, electrochemical, and mechanical properties (FT-IR, SEM, water uptake, IC, IEC, permselectivity, and ionic permeability). And study its performance in the WE system.

2. Material and methods

2.1. Materials

Polyvinylidene fluoride (PVDF, HSV-900, 99.9%) was supplied by Arkema (France), while sodium silicate (Na_2SiO_3, 99.9%) was purchased from SILMACA (Belgium). Dimethyl sulfoxide (DMSO, 99%) and sulfuric acid (H_2SO_4, 96%) were obtained from Biochem Chemopharma (France). Sodium hydroxide (NaOH, 99.9%), sodium chloride (NaCl, 99.99%), and hydrochloric acid (HCl, 37%) were procured from Sigma Aldrich (USA). Additionally, the cation exchange membrane CMI-7000 was sourced from FuMA-Tech (USA). Ag/AgCl electrode, Platinum (Pt) and nickel (Ni) rods with 99.9% purity, supplied from China.

2.2. Membrane preparation

The membrane was prepared by dissolving PVDF and Na_2SiO_3 in DMSO under magnetic stirring at 60 °C for 3 h to obtain a homogeneous brownish gel solution. The resulting solution was then transferred to a hermetically sealed vial and kept at rest for 24 h, allowing complete elimination of air bubbles. The solution was poured onto a clean glass plate using an adjustable film applicator, specifically designed to ensure even distribution and constant membrane thickness. The plate was then placed in an oven at 80 °C for 3 h, ensuring complete evaporation of the solvent and final formation of the membrane film. The film thus formed was carefully detached from the plate and washed thoroughly with deionised water to remove any residual solvent or reagent (Fig. 1). Membranes were prepared with varying concentrations of Na_2SiO_3 added (Table 1). It has been noted that when the concentration of the solution exceeds 1.5%, the solution becomes rigid, thus preventing the formation of a film. The average thickness of the dry membranes was measured at around 35 μm.

2.3. Membrane characterisation

2.3.1. Ionic conductivity IC

The membrane resistance was measured by electrochemical impedance spectroscopy (EIS) using a pot/gal (model EC Lab SP-300). A two-compartment electrochemical cell and graphite electrodes of the same area, separated by the membrane and filled with sodium chloride (NaCl 1 M) solution. The ion conductivity was calculated using the following equation:

$$\sigma = \frac{L}{R_m A} \quad (5)$$

where L is the thickness of the membrane, A is the area of the membrane, and R_m is the resistance of the membrane, respectively.

2.3.2. Water uptake

The membranes (M0 and the optimal) were immersed in deionised water at room temperature for 48 h to ensure complete absorption of water. Following immersion, water on the membrane surface was delicately eliminated using tissue paper. The wetted membranes were then placed in an instrument (SARTORIUOS humidity meter) and heated to 60 °C. The membrane water content was determined when the weight value stabilised. The following equation was used to calculate water

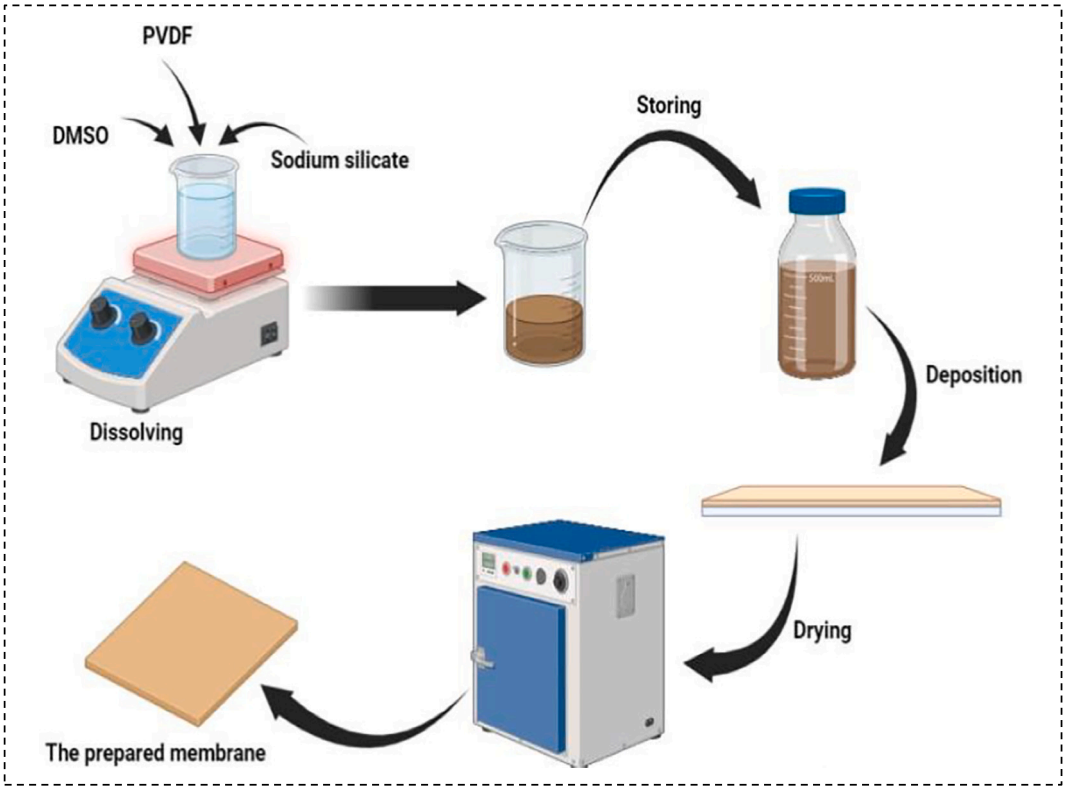

Fig. 1. Schematic illustration of the membrane's preparation method.

Table 1
Composition of membrane components.

Membranes	PVDF wt. (%)	Na_2SiO_3 wt. (%)	DMSO wt. (%)
M0	10	0	90
M1	10	0.5	89.5
M2	10	1	89
M3	10	1.5	88.5

uptake:

$$W_w = \frac{W_{mw} - W_{md}}{W_{md}} \times 100 \quad (6)$$

where W_{mw} and W_{md} are the wet and dry masses of the membranes, respectively.

2.3.3. Permselectivity

Permselectivity was determined using a potentiometric method with an electrochemical cell composed of two compartments (Fig. 2). These compartments, separated by the membrane under study, contained sodium chloride (NaCl) solutions at concentrations of 0.5 M and 0.1 M, respectively. An Ag/AgCl electrode was immersed in each compartment to measure the potential difference between the two electrodes. The experiment was conducted at room temperature, with potential measurements recorded over 30 min, allowing the values to stabilise. The membrane permselectivity $\propto$ is defined as the ratio of measured potential ΔE_m to theoretical potential ΔE_{th} calculated using the equation:

$$\propto = \frac{\Delta E_m}{\Delta E_{th}} \quad (7)$$

The theoretical potential ΔE_{th} was calculated from the Nernst equation:

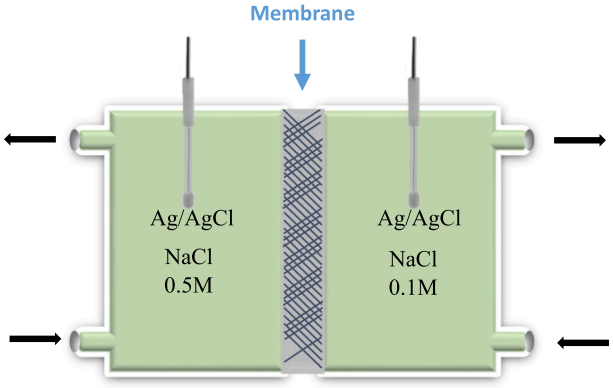

Fig. 2. Schematic illustration of the cell setup for determining membrane permselectivity.

$$\Delta E_{th} = \frac{RT}{F} \ln\left(\frac{a_1}{a_2}\right) \quad (8)$$

where a_1 and a_2 are the activities of the NaCl solutions, F: Faraday constant, R: gas constant and T: temperature.

2.3.4. Ion exchange capacity (IEC)

The modified membrane was cut and rinsed with deionised water to ensure all residues were removed. It was then immersed in a solution of HCl (0.5 M) for 48 h to exchange all cations with H^+, the membrane was carefully rinsed with deionised water to remove excess acid. It was then placed in NaCl solution (0.1 M) for 24 h to enable ion exchange. The solution containing the exchanged ions was recuperated and titrated with a 0.01 M NaOH solution using a pH meter to detect the equivalence point. IEC is calculated by the following equation:

$$IEC\ (meq/g) = \frac{C_{NaOH} \times V_{NaOH}}{W_{md}} \quad (9)$$

where C_{NaOH} and V_{NaOH} are the concentration and the volume of NaOH solution, W_{md} is the dry mass of membrane used.

2.3.5. Permeability

The diffusion coefficient of Na^+ cations was determined using a two-compartment cell separated by the membrane to be studied. One of the two compartments contains a solution of NaCl (0.1 M) and the other contains deionised water (Fig. 3). The solutions in the two compartments have the same volume and are continuously stirred to eliminate concentration polarisation. A conductivity meter was used to measure the conductivity of the solution at regular 20-min intervals. These measurements, as a function of time, were used to determine the concentration of Na^+ in the compartment that initially contained the water. However, the proton diffusion coefficient across the membrane from which Na^+ ions were exchanged by H^+, was determined using the same method employed for Na^+, but the NaCl solution in the first compartment was substituted by HCl (0.1 M) solution. For each of the two ions, the diffusion coefficient (D) was calculated according to the following formula:

$$D = \frac{dC_t}{dt}\frac{VL}{A(C_0 - C_t)} \approx \frac{dC_t}{dt}\frac{VL}{AC_0} \quad (10)$$

where C_0 and C_t are molar concentrations of NaCl or HCl measured at beginning and end of measuring, respectively, A is the effective membrane area, L is the membrane thickness, and V is the volume of the two compartments.

The following equation is used to calculate the ion permeability (P):

$$P = \frac{D}{L} \quad (11)$$

2.3.6. Scanning electron microscopic (SEM)

The surface morphology of the membranes was examined using a scanning electron microscope (SEM Zeiss/Gemini 300). Images were taken for membranes prepared from PVDF without and with modification by Na_2SiO_3. The latter membrane was examined before and after treatment with 1 M NaOH.

2.3.7. Analysis of chemical functional groups (FTIR)

The Fourier-transform infrared (FTIR) spectra of the PVDF-based membranes were obtained using a SHIMADZU 03204 IR spirit spectrophotometer with a resolution of 4 cm^{-1}.

2.3.8. Mechanical strength

A mechanical tensile test was performed in accordance with ASTM D882 using a tensile testing ZWICH/ROELL Z 2.5 machine. Membrane samples, cut into rectangles with standardised dimensions of 1:3 cm, were secured between the movable and fixed jaws and then subjected to a constant tensile rate of 5 mm/min until rupture.

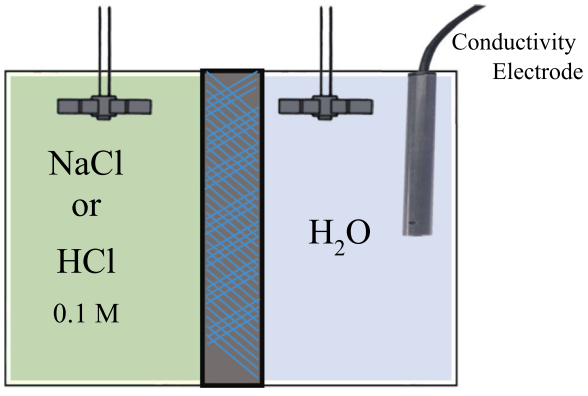

Fig. 3. Schematic representation of diffusion coefficient and permeability measurements.

2.3.9. Membrane application

The membrane, which showed the best electrical performance, was used to separate the two compartments cell during WE. In this section, one of the compartments contains an H_2SO_4 solution (pH = 0), while the other contains NaOH (pH = 14). The electrodes used in this study are Pt for the cathode and Ni for the anode, with identical surfaces equal to 0.2 cm^2. A commercial membrane (CMI-7000) was also tested (Fig. 4a) in order to evaluate the performance of the PVDF-based membrane studied. The results of this study were compared with those obtained in an AE. The latter was performed on the same cell, with and without the studied membrane (Fig. 4b). The series of chronopotentiometry measurements was carried out at a controlled temperature (25 ± 1 °C), applying a current density of 0.1 A/cm^2 using a pot/gal (model ECLab SP-300). The long-term stability of the optimised membrane was assessed over a 50-h operation period, during which the pH of both the anodic and cathodic compartments was monitored throughout electrolysis. The electrolysis voltage was also measured (100 mA/cm^2 applied) and open-circuit conditions (OCV). In addition, the membrane was examined by SEM and FTIR analyses to identify any potential morphological or chemical alterations (Fig. 4a). The experiments were repeated three times to ensure reproducibility of the results.

3. Results and discussion

3.1. Ionic conductivity (IC)

The IC of membranes is the determining factor for a potential application in electrochemistry. The voltage of an electrochemical cell, during water electrolysis, for example, depends on the overvoltages of the electrodes and the ohmic drop. This latter can be of the same order of magnitude as the cell voltage if the membrane resistance is very high, rendering the cell useless. In order to obtain a membrane appropriate for application in the field of water electrolysis, the membranes M0, M1, M2 and M3, mentioned in Table. 1, should be characterised by EIS in order to evaluate their IC. In addition, the IC of the M3A membrane, obtained by sodium hydroxide treatment of the M3 membrane, is evaluated. Fig. 5 shows Nyquist diagrams for membranes M0, M1, M2, M3 and M3A recorded at room temperature in a 1 M NaCl solution. Each plot consists of a capacitive loop at high and medium frequencies and a quasi-vertical line at low frequencies. The semicircle is related to ion transport in the membrane volume, while the linear branch reflects the blocking character of the electrodes. The intersection of the capacitive loop with the real axis at high frequencies indicates the resistance of the NaCl solution [20,29]. The diagram relating to M0 shows a very high membrane resistance (1110 Ω), which corresponds to a very low IC (6.3×10^{-6} S/cm). revealing the insulating properties of this non-modified membrane [30]. On the other hand, the M1 and M2 membranes are characterised by resistances of 142 and 85 Ω respectively, corresponding to specific conductivities of 1.3×10^{-5} and 1.6×10^{-4} S/cm. However, the M3 membrane has a lower resistance, which corresponds to a conductivity of 10^{-3} S/cm. Despite this conductivity, the ohmic drop engendered by this membrane is high, at around 1 V. During electrolysis with such membranes (M1, M2 and M3), the ohmic drop in voltage, when an average current density of 0.1 A/cm^2 is applied, is 3, 2 and 1 V respectively. These values are of the same order of magnitude, or are even higher, than the voltages measured during conventional electrolysis. As a result, these membranes, which are of no interest in the field of membrane electrolysis, are not selected for further characterisation. In order to reduce the membrane resistance, a NaOH treatment is used (1 M for 24 h). The membrane that undergoes this treatment (M3A) shows the lowest capacitive loop, synonymous with the highest IC. Indeed, the

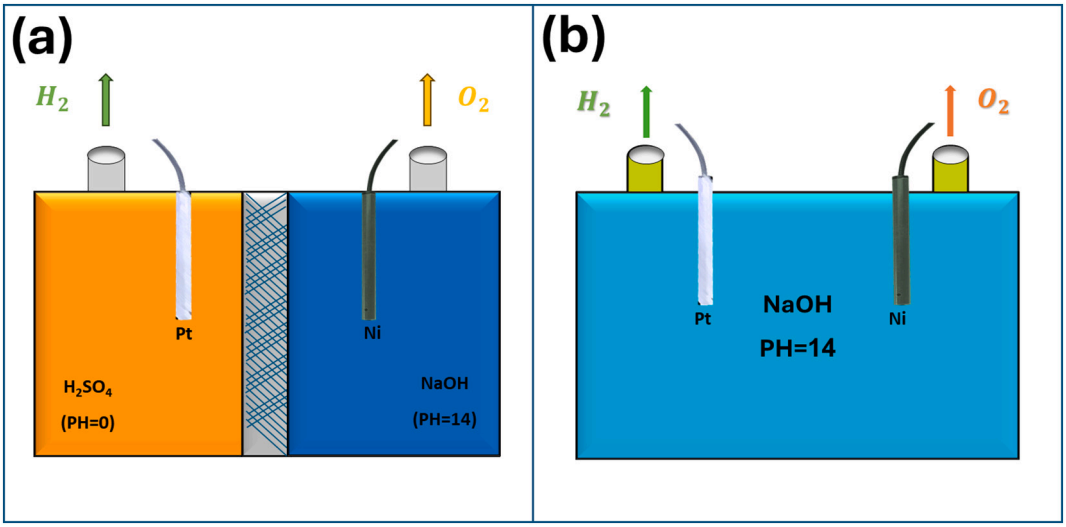

Fig. 4. Schematic of WE cell.

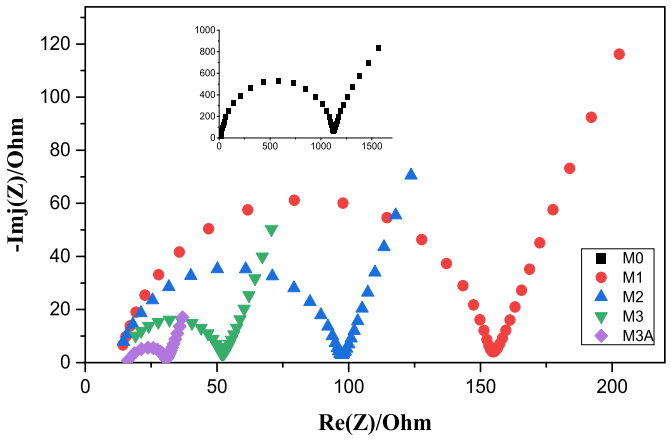

Fig. 5. Nyquist plots for prepared membranes.

resistance of this membrane $< 10\,\Omega$, giving an ohmic drop of just 22 mV. This last pertinent result shows the potential of this membrane in the field of water electrolysis [31]. This membrane therefore merits being characterised by the various techniques mentioned. The IC of M3A is of 2.2×10^{-2} S/cm. Increasing the quantity of silicates (SiO_3^{2-}) added to the polymer leads to an increase in the interaction zones with cations (in this case Na^+), which improves the material's IC [5,32]. Thus, the alkaline treatment of the surface makes the membrane more hydrophilic, which facilitates the rapprochement of Na^+ ions to the M3A surface by improving the ionic transport properties in the membrane and, consequently, the IC. These results are in agreement with those reported in the literature, in particular with the studies of Barbosa et al. [33] who investigated the effect of ionic liquids on the IC of a PVDF-based membrane for lithium-ion batteries and found a value of 2.8 mS/cm^2 for a 15% concentration of ionic liquid.

3.2. Water uptake

The water content analysis of the unmodified M0 and modified M3A polymer membranes reveals distinct physicochemical properties. The unmodified polyvinylidene fluoride (PVDF) membrane exhibited significantly lower water retention capacity (1.08%), a characteristic attributed to its inherent hydrophobic nature [25]. In contrast, the modified membrane demonstrated a marked improvement, achieving 24.8% water content. This improvement is due to the process used: the incorporation of silicate compounds into the polymer matrix facilitates the formation of intermolecular hydrogen bonds, which increases polar interactions with water molecules [34,35]. Alkaline treatment with sodium hydroxide, which M3A underwent, promotes the hydroxyl groups (-OH) (FT-IR analysis) on the membrane surface, thus increasing surface polarity [23].

3.3. Permselectivity

Permselectivity is a property that shows the ability of a membrane to facilitate the movement of counterions (Na^+) while blocking co-ions (Cl^-) [36]. Fig. 6 shows the evolution of the voltage between two Ag/AgCl electrodes, as a function of time, immersed in two NaCl solutions of concentrations equal to 0.1 and 0.5 M. A voltage of around 35 mV (Fig. 6) is recorded when M3A is used between the two solutions. This result indicates that M3A exhibits very high permselectivity, reaching a value of 95%. This permselectivity value is very comparable to those reported in the literature (Table 2) for commercial membranes. This performance can be attributed to the presence of negatively charged functional groups (SiO_3^{2-}) and hydroxide groups after the alkaline treatment. These parameters facilitate electrostatic interactions with cations while blocking the transport of anions, which explains the high

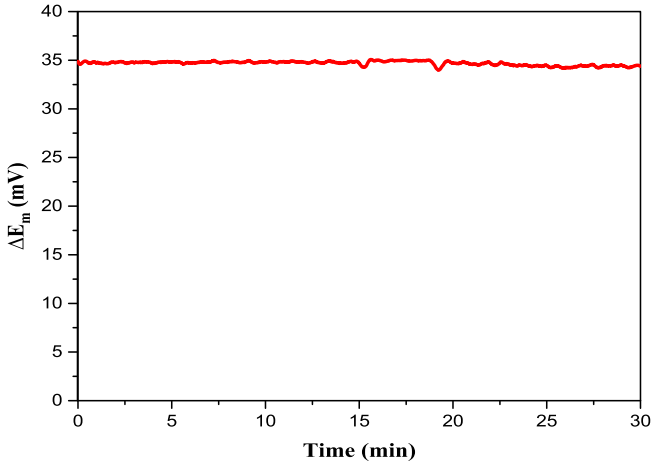

Fig. 6. ΔE_m as a function of time and using reference electrodes across a membrane that separates solutions of different salt concentrations.

Table 2
Permselectivity values of commercial cation exchange membranes.

Membrane	Company	Permselectivity	Reference
Nafion-N117	Dupont	100%	[38]
CEM-Type II	Fujifilm	96%	[39]
CMI-7000	Membrane international Inc	94%	[40]
M3A	–	95%	This work

permselectivity observed [4,37]. On the other hand, when M0 is used to separate the two compartments of the measuring cell, the measured voltage becomes undefined, since this unmodified membrane is insulating.

3.4. Ionic exchange capacity (IEC)

The sodium M3A membrane, used to determine ion exchange capacity, undergoes proton exchange treatment. It was then transferred to a NaCl solution to exchange the protons with Na + ions, which were titrated with NaOH to determine the IEC. The results obtained indicate that the unmodified membrane (M0), due to the absence of co-ions and its hydrophobic nature, does not allow ion exchange. However, the modified membrane M3A shows a relatively high IEC of 0.56 meq/g. This result is in agreement with those reported in the literature [41,42].

3.5. Permeability

Fig. 7 shows the evolution of the permeability, represented by the concentrations of Na^+ and H^+ ions, as a function of time, of the two membranes M3A and M0. The results show that the M0 membrane is impermeable to Na^+ and H^+ ions. This is explained by its hydrophobic nature. However, the permeability of the M3A to H^+ and Na^+ is 2.84 × 10^{-5} cm/s and 1.78 × 10^{-4} cm/s, respectively. In comparison with literature, the proton permeability in the studied membrane is 167 times higher than that of the Nafion 117 membrane, while it is relatively lower than that obtained in the DMPB-TP^+ membrane. On the other hand, the value of sodium ion permeability in the prepared membrane is higher than that obtained in the DMPB-TP^+ membrane [43]. The significant increase in the membrane's permeability has resulted in an improvement in its hydrophilic properties (24.8% water uptake) [44]. The higher permeability of sodium ions compared to protons in a sodium silicate-modified PVDF membrane can be explained by structural modifications to the membrane and specific interactions between ions and groups present in the membrane [45].

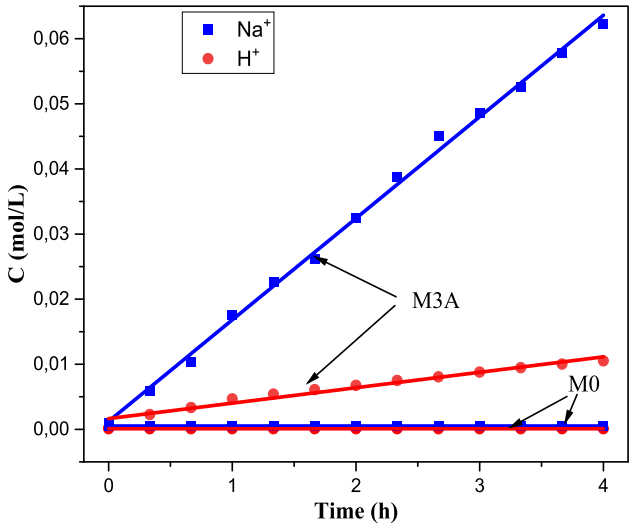

Fig. 7. The diffusion of Na^+ and H^+ through M0 and M3A.

3.6. SEM imaging of the membranes

Scanning electron microscopy (SEM) is used to examine the impact of the modification on the morphology of the polyvinylidene fluoride (PVDF) membrane. The M0 membrane (Fig. 8a) has a relatively homogeneous, rough surface, with a few surface defects due to evaporation of the solvent during membrane preparation. After modification by incorporation of Na_2SiO_3 (Fig. 8b), no change in surface roughness was observed. This shows that the Na_2SiO_3 is completely soluble in the polymer phase and forms a solid solution. However, the defects observed previously are reduced in number and size. This result may be related to the flexibility of this membrane. When the membrane undergoes surface treatment with NaOH (Fig. 8c), the roughness is remarkably reduced. This indicates the effectiveness of this treatment in making the membrane surface hydrophilic. This result supports those of IC and water retention.

3.7. Analysis of chemical functional groups (FTIR)

FTIR analysis of the prepared membranes (Fig. 9), for M0 that gives PVDF polymer spectrometer reveals the coexistence of α, β and γ crystalline phases, identified by characteristic bands: α phase by bending vibration CF_2 at 760 cm^{-1}, β phase by rocking CH_2 at 838 cm^{-1} and out-of-plane deformation CF_2 at 1272 cm^{-1}, and γ phase by bands at 480 cm^{-1} and 1236 cm^{-1} (CF out-of-plane deformation). Additional vibrations at 880 cm^{-1} (CH bending), 1070 cm^{-1} (C—C stretching), 1180 cm^{-1} (CF_2 stretching), 1406 cm^{-1} (CH_2 deformation) and 2980:3020 cm^{-1} (CH_2 stretches) [33].

For M3A, the PVDF bands persist, while two new regions appear: a broad band centred between 1050 and 1100 cm^{-1}, assigned to Si-O-Si asymmetric elongation vibrations characteristic of inorganic modification, and a broader band in the 3300–3600 cm^{-1} range, associated with stretching vibration -OH groups [32,35,46].

3.8. Mechanical strength

The tensile strength of M3A reached 45.6 ± 2.10 MPa and an elongation at break of 25.1%, which are higher than those of the pure PVDF membrane (23.5 ± 1.7 MPa and 21%). This improvement is due to the structural interaction between the polymer matrix (PVDF) and the added inorganic particles. The addition of Na_2SiO_3 contributes to the formation of a more homogeneous structure, which reduces defects and increases the density of the material [47,48].

3.9. Membrane application

The M3A membrane, which has shown remarkable characteristics, is chosen for application in the field of water electrolysis. Firstly, an alkaline electrolysis in a NaOH solution (pH ≈ 14) is effected for 15 min at 0.1 A/cm^2 using a Ni positive electrode and a Pt negative electrode. The curve for this electrolysis in Fig. 10a is characterised by a jump in voltage, due to the ohmic drop and overvoltage, in the first few moments, then the voltage tends to be relatively stable at around 2.68 V [49]. This value, which is relatively high, is logical since the electrolysis conditions (temperature, pressure, etc.) have not yet been optimised [13]. M3A is then inserted to separate the two compartments in the previous cell, maintaining the same conditions. The curve for electrolysis with a membrane is identical to that for alkaline electrolysis without a membrane. However, the membrane electrolysis voltage remains stable at around 2.70 V. The difference between this value and that of electrolysis without a membrane, which is of the order of 20 mV, is due to the resistance of the membrane. This latter value supports the results of the study of the IC of M3A [10].

For another series of experiments, M3A is used to study its performance in the DE system (the effect of migration and chemical diffusion of ions, particularly H^+, across this membrane). This membrane is used

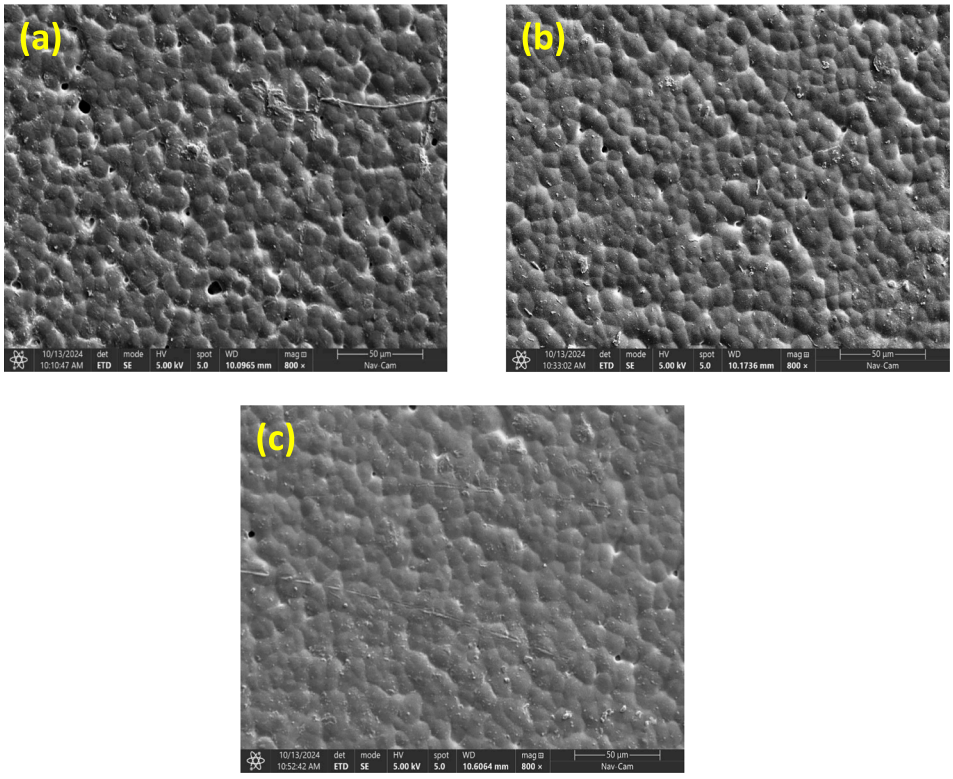

Fig. 8. SEM images of membranes **(a)** M0, **(b)** M3, and **(c)** M3A.

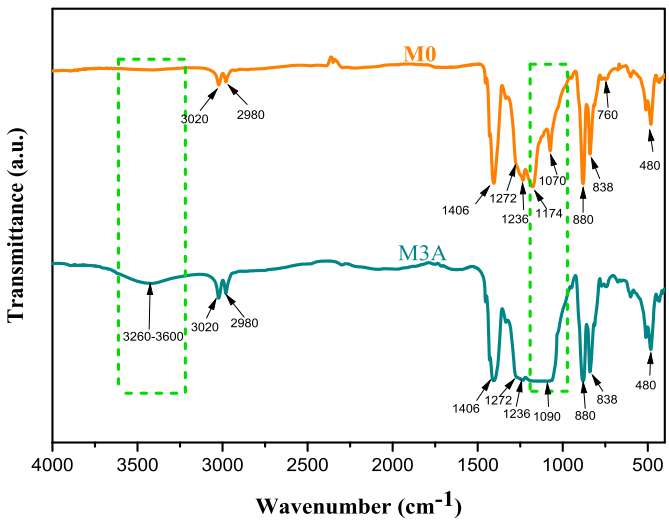

Fig. 9. FTIR spectra of the pristine PVDF membrane (M0) and the modified (M3A).

to separate the two compartments, filled with two solutions of different pH, catholyte (pH 0) and anolyte (pH 14). The curves (0–240 min) in Fig. 10b have a similar appearance to the curves in Fig. 10a. The curve of the first electrolysis applied (0 min), relating to electrolysis conducted just after the cell compartments have been filled, shows an electrolysis voltage that rises progressively from 1.20 to 1.43 V. A reduction in energy consumption of ~50% has been achieved. This shows the effectiveness of the DE system [16]. After this electrolysis, the system was maintained at zero current for a fixed period (30, 60, 120, and 240 min) in order to evaluate the diffusion of ions across the membrane in the absence of the electric field. After each period, a new 15 min electrolysis was completed and compared with the previous one to see any changes due to diffusion through M3A (pH of electrolytes). The curves recorded respectively after 30, 60, 120 and 240 min of current cut-off are practically superimposable with the curve of the first electrolysis conducted. This shows that ionic diffusion is practically 0. The same experiments were carried out for commercial membrane CMI-7000 to compare the performance of M3A. The curves are shown in Fig. 10c that electrolysis with such a membrane is less efficient than that with M3A, since its electrolysis voltage rises to 1.8 V (at 0 min of 0 A applied) [19]. This increase in voltage, compared with that of M3A, is probably due to the ohmic drop in the commercial membrane [50]. In fact, the resistance of this membrane is 18 Ω and generates, for an electrolysis current density of 0.1 A/cm^2, an ohmic drop of around 350 mV. After power cuts of 30 and 60 min, the electrolysis voltages became around 1.9 and 2.1 V, corresponding to voltage increases of 100 and 200 mV, respectively. This change is explained by the effect of diffusion of H^+ ions (neutralisation of electrolytes) through CMI 7000, which causes a reduction in the pH difference between the two compartments, thereby increasing the electrolysis voltage. After 120 min of current cut-off, the electrolysis voltage approaches 3 V, indicating that the commercial membrane is becoming more permeable to H^+ [18].

Long-term evaluation of the membrane in a DEWE cell over a period of 50 h revealed excellent chemical and electrochemical stability. pH measurements taken in the anodic and cathodic compartments before and after the test showed no significant variation (Fig. 11a), demonstrating the membrane's effectiveness in preventing electrolyte cross-mixing. At the same time, the OCV remained constant in the absence of current, while under polarisation, the cell voltage remained stable (Fig. 11b) within a narrow range (1.42–1.51 V) [18,19]. The SEM images (Fig. 12) reveal a complete absence of morphological degradation, attesting to the structural integrity of the membrane after 50 h of operation and the FTIR spectrum in Fig. 13 is identical to that of M3A in Fig. 9, with no characteristic bands disappearing or appearing. This confirms the absence of chemical degradation and the structural stability of the membrane between acidic and alkaline conditions [51]. These results confirm that PVDF is an intrinsically stable polymer matrix

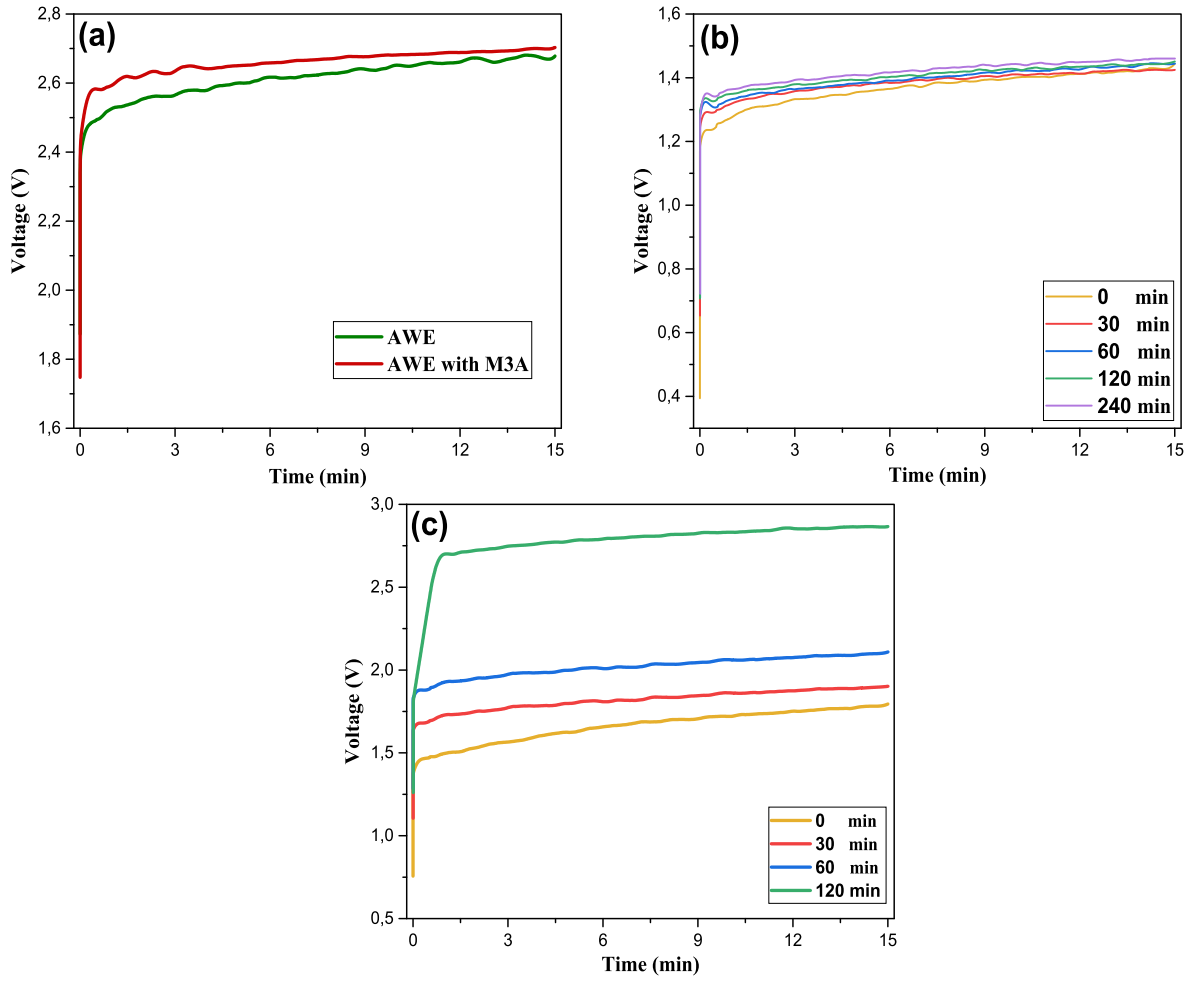

Fig. 10. Chronopotentiogram recorded for WE systems **(a)** AWE, **(b)** DE with M3A, and **(c)** DE with CMI-7000.

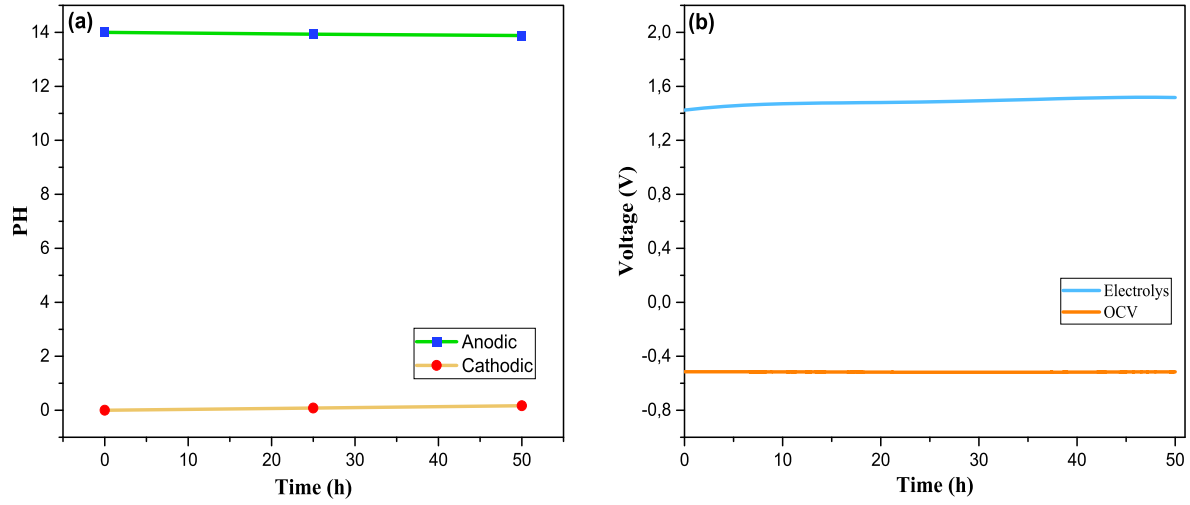

Fig. 11. Stability test of M3A **(a)** PH measure, **(b)** Chronopotentiogram and OCV curve.

and that the modification significantly improved its electrochemical performance without compromising its chemical integrity or structural stability under operating conditions [21].

4. Conclusion

A PVDF membrane modified with Na_2SiO_3 was prepared and characterised by various techniques. All the characterisations show the effect of this modifier. The membrane prepared by adding 15% (based on the weight of the polymer) of Na_2SiO_3 to PVDF with an alkaline surface

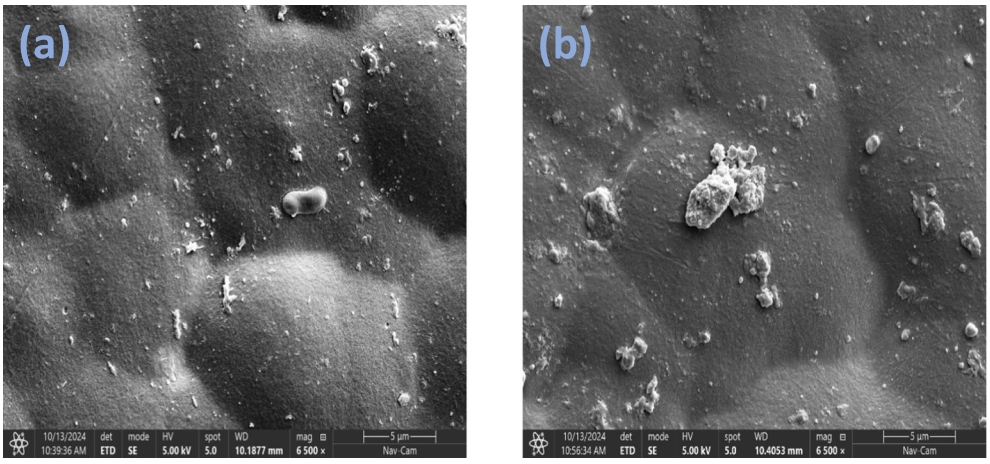

Fig. 12. SEM of membrane M3A **(a)** before and **(b)** after electrolysis.

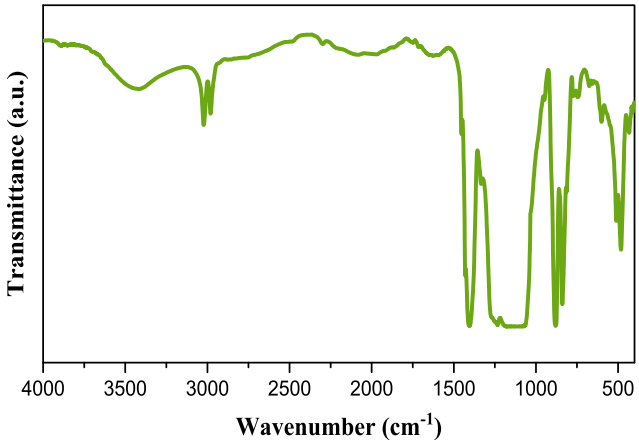

Fig. 13. The FTIR spectra of M3A after electrolysis.

treatment (M3A) shows the best characteristics, such as IEC = 0.56 meq/g, permselectivity = 95%, IC = 2.2×10^{-2} S/cm, and high permeability for Na^+ 1.78×10^{-4} cm/s. These performances make this membrane a potential choice in the field of water electrolysis. M3A's characteristics ensure the migration of cations during water electrolysis while blocking the diffusion of protons after the current has been cut off. During electrolysis in a two-compartment cell with different pH values (0 and 14), the electrolysis voltage is less than 1.5 V at 0.1 A/cm^2. The membrane also exhibited mechanical strength 45.6 MPa, as confirmed by tensile testing, and remarkable operational stability over 50 h, with no significant degradation in voltage, pH of electrolytes, morphology (SEM), or chemical structure (FTIR). The overall results obtained by this membrane are comparable to and better than those of commercial membranes CMI-7000.

CRediT authorship contribution statement

Soheyb Khadraoui: Writing – review & editing, Writing – original draft, Visualization, Validation, Software, Methodology, Investigation, Formal analysis, Data curation, Conceptualization. **Kamel Noufel:** Writing – review & editing, Writing – original draft, Supervision. **Laid Telli:** Writing – review & editing, Writing – original draft, Validation, Supervision. **Alberto Figoli:** Writing – review & editing.

Consent to participate

All authors have given their consent to participate in submitting this manuscript to this journal.

Ethics approval

We declare that all ethical guidelines for authors have been followed by all authors.

Funding

The authors declare that no funds were received to support this research.

Declaration of competing interest

The authors declare that they have no known competing financial interests or personal relationships that could have appeared to influence the work reported in this paper.

Acknowledgments

The authors would like to express their gratitude to the higher education and scientific research ministry for their support, especially CRAPC for SEM imaging. The authors thank the department of chemistry, university of M'sila for providing the FTIR analysis.

Data availability

Data will be made available on request.

References

[1] A.M. Khan, F. Russo, F. Macedonio, A. Criscuoli, E. Curcio, A. Figoli, The state of the art on PVDF membrane preparation for membrane distillation and membrane crystallization: towards the use of non-toxic solvents, Membranes 15 (2025) 1–26, https://doi.org/10.3390/membranes15040117.
[2] Z. Abdorrezaee, C. Falamaki, Simultaneous polymerization, crosslinking, and preparation of a smart nanocomposite membrane for desalination pervaporation by a novel and green photocatalytic method, Sep. Purif. Technol. 378 (2025) 134530, https://doi.org/10.1016/J.SEPPUR.2025.134530.
[3] K.G. Motora, C.M. Wu, W.H. Lee, Y.T. Peng, Scalable preparation of carbon fabric Janus membrane for water evaporation, photothermal conversion, sewage treatment, and desalination applications and its practical application, Sep. Purif. Technol. 375 (2025) 133830, https://doi.org/10.1016/J.SEPPUR.2025.133830.
[4] D.V. Golubenko, R.R. Shaydullin, A.B. Yaroslavtsev, Improving the conductivity and permselectivity of ion-exchange membranes by introduction of inorganic oxide nanoparticles: impact of acid–base properties, Colloid Polym. Sci. 297 (2019) 741–748, https://doi.org/10.1007/s00396-019-04499-1.
[5] Ö. Tekinalp, P. Zimmermann, S. Holdcroft, O.S. Burheim, Cation Exchange Membranes and Process Optimizations in Electrodialysis for Selective Metal Separation : A Review, 2023.

[6] M. del M. Cerrillo-Gonzalez, M. Villen-Guzman, J.M. Rodriguez-Maroto, J.M. Paz-Garcia, Metal recovery from wastewater using electrodialysis separation, Metals 14 (2024), https://doi.org/10.3390/met14010038.
[7] J. Hao, Y. Jiang, X. Gao, W. Lu, Y. Xiao, Z. Shao, B. Yi, Functionalization of polybenzimidazole-crosslinked poly(vinylbenzyl chloride) with two cyclic quaternary ammonium cations for anion exchange membranes, J. Membr. Sci. 548 (2018) 1–10, https://doi.org/10.1016/J.MEMSCI.2017.10.062.
[8] S.A. Grigoriev, V.N. Fateev, D.G. Bessarabov, P. Millet, Current status, research trends, and challenges in water electrolysis science and technology, Int. J. Hydrog. Energy 45 (2020) 26036–26058, https://doi.org/10.1016/j.ijhydene.2020.03.109.
[9] J. Hao, Y. Jiang, X. Gao, F. Xie, Z. Shao, B. Yi, Degradation reduction of polybenzimidazole membrane blended with CeO2 as a regenerative free radical scavenger, J. Membr. Sci. 522 (2017) 23–30, https://doi.org/10.1016/J.MEMSCI.2016.09.010.
[10] O. Racchi, R. Baldassari, E. Araya-Hermosilla, V. Mattoli, P. Minei, A. Pozio, A. Pucci, Polyketone-based anion-exchange membranes for alkaline water electrolysis, Polymers 15 (2023) 1–12, https://doi.org/10.3390/polym15092027.
[11] J. Chi, H. Yu, Water electrolysis based on renewable energy for hydrogen production, Cuihua Xuebao/Chinese, J. Catal. 39 (2018) 390–394, https://doi.org/10.1016/S1872-2067(17)62949-8.
[12] J.M. Gohil, K. Dutta, Structures and properties of polymers in ion exchange membranes for hydrogen generation by water electrolysis, Polym. Adv. Technol. 32 (2021) 4598–4615, https://doi.org/10.1002/pat.5482.
[13] J.C. Ehlers, A.A. Feidenhans'l, K.T. Therkildsen, G.O. Larrazábal, Affordable green hydrogen from alkaline water electrolysis: key research needs from an industrial perspective, ACS Energy Lett. 8 (2023) 1502–1509, https://doi.org/10.1021/acsenergylett.2c02897.
[14] M. Wang, Z. Wang, X. Gong, Z. Guo, The intensification technologies to water electrolysis for hydrogen production - a review, Renew. Sust. Energ. Rev. 29 (2014) 573–588, https://doi.org/10.1016/j.rser.2013.08.090.
[15] M.A. Khan, H. Zhao, W. Zou, Z. Chen, W. Cao, J. Fang, J. Xu, L. Zhang, J. Zhang, Recent Progresses in Electrocatalysts for Water Electrolysis, Springer Singapore, 2018, https://doi.org/10.1007/s41918-018-0014-z.
[16] M.Y. Lin, L.W. Hourng, K.L. Chiou, Parametric analysis of water electrolysis by dual electrolytes and cells, Int. J. Green Energy 16 (2019) 293–298, https://doi.org/10.1080/15435075.2018.1564139.
[17] B. Liu, G. Wang, X. Feng, L. Dai, Z. Wen, S. Ci, Energy-saving H2 production from a hybrid acid/alkali electrolyzer assisted by anodic glycerol oxidation, Nanoscale 14 (2022) 12841–12848, https://doi.org/10.1039/D2NR02689A.
[18] L. Lee, D. Kim, Poly(arylene ether ketone)-based bipolar membranes for acid-alkaline water electrolysis applications, J. Mater. Chem. A 9 (2021) 5485–5496, https://doi.org/10.1039/d0ta09398j.
[19] J. Xu, I. Amorim, Y. Li, J. Li, Z. Yu, B. Zhang, A. Araujo, N. Zhang, L. Liu, Stable overall water splitting in an asymmetric acid/alkaline electrolyzer comprising a bipolar membrane sandwiched by bifunctional cobalt-nickel phosphide nanowire electrodes, Carbon Energy 2 (2020) 646–655, https://doi.org/10.1002/cey2.56.
[20] J.E. Park, S.Y. Kang, S.H. Oh, J.K. Kim, M.S. Lim, C.Y. Ahn, Y.H. Cho, Y.E. Sung, High-performance anion-exchange membrane water electrolysis, Electrochim. Acta 295 (2019) 99–106, https://doi.org/10.1016/j.electacta.2018.10.143.
[21] D.V. Golubenko, O.V. Korchagin, D.Y. Voropaeva, V.A. Bogdanovskaya, A. B. Yaroslavtsev, Membranes based on polyvinylidene fluoride and radiation-grafted sulfonated polystyrene and their performance in proton-exchange membrane fuel cells, Polymers 14 (2022), https://doi.org/10.3390/polym14183833.
[22] H. Wu, S.J. Liu, K. Lian, Aqueous based dual-electrolyte rechargeable Pb–Zn battery with a 2.8 V operating voltage, J. Energy Storage 29 (2020) 101305, https://doi.org/10.1016/j.est.2020.101305.
[23] Z. Xu, G. Ma, D. Rana, T. Matsuura, C.Q. Lan, Modification of exterior and intraporous surfaces of polyvinylidene fluoride membranes using KOH/water/alcohol ternary: effects of wettability, polarity, and OH− activity, React. Funct. Polym. 208 (2025) 106147, https://doi.org/10.1016/J.REACTFUNCTPOLYM.2024.106147.
[24] J. Cao, Z. Yuan, X. Li, W. Xu, H. Zhang, Hydrophilic poly(vinylidene fluoride) porous membrane with well connected ion transport networks for vanadium flow battery, J. Power Sources 298 (2015) 228–235, https://doi.org/10.1016/j.jpowsour.2015.08.067.
[25] G. Dong Kang, Y. Ming Cao, Application and modification of poly(vinylidene fluoride) (PVDF) membranes - a review, J. Membr. Sci. 463 (2014) 145–165, https://doi.org/10.1016/j.memsci.2014.03.055.
[26] C. Sun, X. Feng, Enhancing the performance of PVDF membranes by hydrophilic surface modification via amine treatment, Sep. Purif. Technol. 185 (2017) 94–102, https://doi.org/10.1016/j.seppur.2017.05.022.
[27] A. Siekierka, M. Bryjak, Modified poly(vinylidene fluoride) by diethylenetriamine as a supported anion exchange membrane for lithium salt concentration by hybrid capacitive deionization, Membranes 12 (2022), https://doi.org/10.3390/membranes12020103.
[28] S. Mishra, J. Sharma, P. Upadhyay, V. Kulshrestha, Investigation on sturdy centipede-configured PVDF based proton exchange membrane for water electrolysis, J. Membr. Sci. 708 (2024) 123022, https://doi.org/10.1016/J.MEMSCI.2024.123022.
[29] L. Luo, K. Ma, X. Song, Y. Zhao, J. Tang, Z. Zheng, J. Zhang, A magnesium carbonate hydroxide nanofiber/poly(vinylidene fluoride) composite membrane for high-rate and high-safety lithium-ion batteries, Polymers 15 (2023), https://doi.org/10.3390/polym15204120.
[30] B. Li, Q. Su, L. Yu, W. Liu, S. Dong, S. Ding, M. Zhang, G. Du, B. Xu, Biomimetic PVDF/LLTO composite polymer electrolyte enables excellent interface contact and enhanced ionic conductivity, Appl. Surf. Sci. 541 (2021) 148434, https://doi.org/10.1016/j.apsusc.2020.148434.
[31] X. Wang, Z. Fang, M. Zhang, S. Xie, D. Xie, P. Liu, S. Wang, F. Cheng, T. Xu, Macromolecular crosslinked poly(aryl piperidinium)-based anion exchange membranes with enhanced ion conduction for water electrolysis, J. Membr. Sci. 700 (2024) 122717, https://doi.org/10.1016/J.MEMSCI.2024.122717.
[32] S. Battery, P. Arjunan, M. Kouthaman, R. Subadevi, Superior Ionic Transferring Polymer with Silicon Dioxide Composite Membrane via Phase Inversion Method Designed for High Performance, 2020, pp. 1–11.
[33] J.C. Barbosa, D.M. Correia, R. Gonçalves, V. de Zea Bermudez, M.M. Silva, S. Lanceros-Mendez, C.M. Costa, Enhanced ionic conductivity in poly(vinylidene fluoride) electrospun separator membranes blended with different ionic liquids for lithium ion batteries, J. Colloid Interface Sci. 582 (2021) 376–386, https://doi.org/10.1016/j.jcis.2020.08.046.
[34] Z.H. Huang, X. Zhang, Y.X. Wang, J.Y. Sun, H. Zhang, W.L. Liu, M.P. Li, X.H. Ma, Z. L. Xu, Fe3O4/PVDF catalytic membrane treatment organic wastewater with simultaneously improved permeability, catalytic property and anti-fouling, Environ. Res. 187 (2020) 109617, https://doi.org/10.1016/j.envres.2020.109617.
[35] B. Saini, M.K. Sinha, Synergetic effects of organic and inorganic additives on improvement in hydrophilicity and performance of PVDF antifouling ultrafiltration membrane for removal of natural organic material from water, J. Appl. Polym. Sci. 138 (2021), https://doi.org/10.1002/app.50568.
[36] F. Radmanesh, T. Rijnaarts, A. Moheb, M. Sadeghi, W.M. de Vos, Enhanced selectivity and performance of heterogeneous cation exchange membranes through addition of sulfonated and protonated montmorillonite, J. Colloid Interface Sci. 533 (2019) 658–670, https://doi.org/10.1016/j.jcis.2018.08.100.
[37] S.B.B. Solberg, P. Zimmermann, Ø. Wilhelmsen, R. Bock, O.S. Burheim, Analytical treatment of ion-exchange permselectivity and transport number measurements for high accuracy, J. Membr. Sci. 685 (2023) 121904, https://doi.org/10.1016/j.memsci.2023.121904.
[38] A.H. Avci, D.A. Messana, S. Santoro, R.A. Tufa, E. Curcio, G. Di Profio, E. Fontananova, Energy harvesting from brines by reverse electrodialysis using nafion membranes, Membranes 10 (2020) 1–16, https://doi.org/10.3390/membranes10080168.
[39] E. Altıok, T.Z. Kaya, E. Güler, N. Kabay, M. Bryjak, Performance of reverse electrodialysis system for salinity gradient energy generation by using a commercial ion exchange membrane pair with homogeneous bulk structure, Water (Switzerland) 13 (2021), https://doi.org/10.3390/w13060814.
[40] P. Vadthya, A. Kumari, C. Sumana, S. Sridhar, Electrodialysis aided desalination of crude glycerol in the production of biodiesel from oil feed stock, Desalination 362 (2015) 133–140, https://doi.org/10.1016/j.desal.2015.02.001.
[41] A. Alabi, L. Cseri, A. Al Hajaj, G. Szekely, P. Budd, L. Zou, Graphene-PSS/l-DOPA nanocomposite cation exchange membranes for electrodialysis desalination, Environ. Sci. Nano 7 (2020) 3108–3123, https://doi.org/10.1039/d0en00496k.
[42] E. Jashni, S.M. Hosseini, High selective heterogeneous cation exchange membrane modified by l-cysteine with enhanced electrochemical performance, Ionics 26 (2020) 875–894, https://doi.org/10.1007/s11581-019-03253-5.
[43] J. Zhou, Y. Liu, P. Zuo, Y. Li, Y. Dong, L. Wu, Z. Yang, T. Xu, Highly conductive and vanadium sieving microporous Tröger's base membranes for vanadium redox flow battery, J. Membr. Sci. 620 (2021) 118832, https://doi.org/10.1016/j.memsci.2020.118832.
[44] J. Kamcev, D.R. Paul, G.S. Manning, B.D. Freeman, Ion diffusion coefficients in ion exchange membranes: significance of counterion condensation, Macromolecules 51 (2018) 5519–5529, https://doi.org/10.1021/acs.macromol.8b00645.
[45] S.M. Hosseini, Z. Ahmadi, M. Nemati, F. Parvizian, S.S. Madaeni, Electrodialysis heterogeneous ion exchange membranes modified by SiO2 nanoparticles: fabrication and electrochemical characterization, Water Sci. Technol. 73 (2016) 2074–2084, https://doi.org/10.2166/wst.2016.030.
[46] V.I. Ak Suel, M.H. Rohalin, N. Misdan, Preparation of graphene oxide (GO) incorporated-polyvinylidene fluoride (PVDF) nanofiltration membrane with alkaline post-treatment for textile wastewater treatment, J. Appl. Membr. Sci. Technol. 28 (2024) 103–111, https://doi.org/10.11113/amst.v28n2.291.
[47] H.-Y. Lin, Y.-J. Kuo, S.-H. Chang, Electrospinning of nanofibers chitosan/PVA-sodium silicate characterization of electrospun nanofiber matrices made of collagen blends as potential skin substitutes, J. Phys. Conf. Ser. (2021) 32012, https://doi.org/10.1088/1742-6596/1918/3/032012.
[48] D.I. Lee, Y.H. Ha, H. Jeon, S.H. Kim, Preparation and properties of polyurethane composite foams with silica-based fillers, Appl. Sci. 12 (2022) 7418, https://doi.org/10.3390/APP12157418.
[49] H. Tü Ysü, (UTC). Reaction, Angew. Chem. Int. Ed. 57 (2024) 24, https://doi.org/10.1021/acs.accounts.3c00709.
[50] X. Yan, X. Yang, X. Su, L. Gao, J. Zhao, L. Hu, M. Di, T. Li, X. Ruan, G. He, Twisted ether-free polymer based alkaline membrane for high-performance water electrolysis, J. Power Sources 480 (2020) 228805, https://doi.org/10.1016/j.jpowsour.2020.228805.
[51] J. Hao, X. Gao, Y. Jiang, H. Zhang, J. Luo, Z. Shao, B. Yi, Crosslinked high-performance anion exchange membranes based on poly(styrene-b-(ethylene-co-butylene)-b-styrene), J. Membr. Sci. 551 (2018) 66–75, https://doi.org/10.1016/J.MEMSCI.2018.01.033.